

## Angular Distribution of Inclusive Lepton Pairs from Heavy Quarkonium Decay

Jürgen G. Körner

Johannes Gutenberg-Universität Mainz, D-6500 Mainz, Federal Republic of Germany

Douglas W. McKay

University of Kansas, Lawrence, KS 66045, USA

Received 4 January 1983; in revised form 19 May 1983

**Abstract.** We calculate polar and azimuthal angular distributions of inclusive lepton pairs in the decay  $Q\bar{Q}(1^{--}) \rightarrow 1^+ 1^- + X$  from the first order QCD process  $Q\bar{Q}(1^{--}) \rightarrow 1^+ 1^- + gg$ . We provide opening angle distributions of the lepton pair in order to assess the measurability of the lepton pairs.

We suggest a measurement of the angular distributions of the lepton pair in the inclusive lepton pair decay of heavy quarkonium resonances  $Q\bar{Q}(1^{--}) \rightarrow 1^+ 1^- + X$ . To lowest order in QCD the decay proceeds via  $Q\bar{Q}(1^{--}) \rightarrow 1^+ 1^- + gg$  as drawn in Fig. 1 [1, 2]. Although rates are small, two of the proposed measurements offer the opportunity to test QCD from leptonic measurements alone.

The differential decay rate of a heavy quarkonium resonance into a lepton pair and two gluons is given by

$$\frac{d\Gamma(Q\bar{Q}(1^{--}) \rightarrow l^+ l^- + g_2 + g_3)}{dq^2 dx_q dx_2 d\varphi^* d\cos\Theta^*} = \frac{\alpha^2 \alpha_s^2 e_Q^2}{108\pi} \cdot \frac{M^2 |\Psi(0)|^2}{q^2} \frac{3}{8\pi} \left(1 - \frac{4m_l^2}{q^2}\right)^{1/2} \cdot \left\{ \mathcal{H}_{++} \left( (1 + \cos^2 \Theta^*) + \frac{4m_l^2}{q^2} \sin^2 \Theta^* \right) + \mathcal{H}_{00} \left( \sin^2 \Theta^* + \frac{4m_l^2}{q^2} \cos^2 \Theta^* \right) + \mathcal{H}_{+-} \sin^2 \Theta^* \cos 2\varphi^* \left( 1 - \frac{4m_l^2}{q^2} \right) + 2\sqrt{2} \operatorname{Re} \mathcal{H}_{+0} \sin 2\Theta^* \cos \varphi^* \left( 1 - \frac{4m_l^2}{q^2} \right) \right\} \quad (1)$$

where  $M$  and  $m_l$  are the quarkonium and lepton mass,  $e_Q$  the charge of its constituent quark,  $\Psi(0)$  its wave

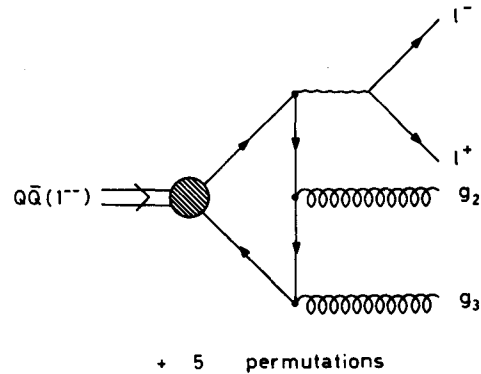


Fig. 1. Lowest order diagrams contributing to  $Q\bar{Q}(1^{--}) \rightarrow 1^+ 1^- + gg$

function at origin,  $q^2$  the virtuality of the photon and the  $x_i$  are the scaled energies  $x_i = 2E_i/M$  of the virtual photon ( $i = q$ ) and gluons ( $i = 2, 3$ ) in the quarkonium rest system ( $x_q + x_2 + x_3 = 2$ ).  $\Theta^*$  and  $\varphi^*$  are the polar angle (relative to the virtual photon's momentum direction) and azimuthal angle (relative to the  $\gamma^* gg$  plane) of the negatively charged lepton in the rest system of the virtual photon. The case where the azimuth is defined relative to the beam-virtual photon plane will be discussed later. The  $\mathcal{H}_{mm'}$  are the helicity projections of the hadron tensor  $\mathcal{H}_{mm'} = \epsilon_\mu^{*m} \mathcal{H}_{\mu\nu} \epsilon_\nu^{m'}$  which is given by the square of the amplitude  $A(Q\bar{Q} \rightarrow \gamma^*(\mu)g_2g_3)$  summed over the quarkonium and gluon spins. The total spin sum of the squared amplitude is given by  $2\mathcal{H}_{++} + \mathcal{H}_{00} = \mathcal{H}_{\mu\mu}$  and corresponds to the  $|A|^2$  of [1].

The hadron tensor  $\mathcal{H}_{\mu\nu}$  was calculated by hand from the Feynman diagrams Fig. 1. One obtains

$$\mathcal{H}_{\mu\nu} = H_1 \hat{g}_{\mu\nu} + H_2 \hat{p}_{2\mu} \hat{p}_{2\nu} + H_3 \hat{p}_{3\mu} \hat{p}_{3\nu} + H_4 (\hat{p}_{2\mu} \hat{p}_{3\nu} + \hat{p}_{2\nu} \hat{p}_{3\mu}) \quad (2)$$

where we use the gauge invariant covariant forms  $\hat{g}_{\mu\nu} = g_{\mu\nu} - q_\mu q_\nu / q^2$  and  $\hat{p}_i = p_i - (p_i q / q^2) q$ . The invariants  $H_i$  in the expansion (2) are given by

$$\begin{aligned} H_1 &= 2((c^2 - x_2 x_3)^2 + rc(2c - (3-r)x_2 x_3))N \\ H_2 &= 4(b^2(1-r) + 2rc^2)N/M^2 \\ H_3 &= 4(a^2(1-r) + 2rc^2)N/M^2 \\ H_4 &= 4(-ab(1-r) + r(1-r)(c + x_2 x_3))N/M^2 \end{aligned} \quad (3)$$

where  $N = 2^8((x_q - 2r)x_2 x_3 M^2)^{-2}$  and  $a = 1 - x_3 - r$ ,  $b = 1 - x_2 - r$ ,  $c = 1 - x_q + r$  and  $r = q^2/M^2$ .

The angle integrated rate is determined by  $2\mathcal{H}_{++} + \mathcal{H}_{00} = \mathcal{H}_{\mu\mu}$  for which one obtains from (2)

$$\begin{aligned} \mathcal{H}_{\mu\mu} &= 2N\{3(c^2 - x_2 x_3)^2 + 3rc(2c - (3-r)x_2 x_3) \\ &\quad - c^2(a^2 + b^2 - 2r(1-r)) \\ &\quad - (1-r)(3abc + x_2 x_3(ab - 2rc))\} \end{aligned} \quad (4a)$$

In the  $r=0$  limit (4a) reduces to the Ore-Powell formula

$$\begin{aligned} \mathcal{H}_{\mu\mu} &= 2N(r=0) \\ &\cdot \{x_q^2(1-x_q)^2 + x_2^2(1-x_2)^2 + x_3^2(1-x_3)^2\} \end{aligned} \quad (4b)$$

The trace of the hadron tensor (4a) agrees with the expressions given in [1, 2]. Note that the symmetrical appearance of the first terms in  $H_2$ ,  $H_3$  and  $H_4$  is due to the particular expansion chosen in (2) and necessary for  $\mathcal{H}_{\mu\mu}$  to behave smoothly as  $r \rightarrow 0$ .

In Fig. 2 we plot the normalized differential decay rate for  $\Psi \rightarrow e^+ e^- + gg$ . The decay spectrum is very much peaked towards small  $q^2$ -values close to the photon pole and quickly falls off toward the phase space limit  $r=1$  due to the combined effect of moving away from the photon pole and the narrowing down of phase space ( $\sim (1-r)^3$  as  $r \rightarrow 1$ ). In Fig. 2 we have also included the Real-Photon-Approximation (RPA) rate which is obtained by setting  $\mathcal{H}_{\mu\mu}(q^2) = \mathcal{H}_{\mu\mu}(0)$ . Note that the approximate RPA-rate falls much more steeply than the exact rate. For the RPA-rate one finds, after integrating in the appropriate phase space domain

$$\begin{aligned} \frac{1}{2}(2 - x_q - \sqrt{x_q^2 - 4r}) &\leq x_2 \leq \frac{1}{2}(2 - x_q + \sqrt{x_q^2 - 4r}), \\ 2\sqrt{r} &\leq x_q \leq 1 + r, \\ r_i (= 4m^2/M^2) &\leq r \leq 1, \end{aligned} \quad (5)$$

$$\begin{aligned} \Gamma^{-1} \frac{d\Gamma}{dr} &= \tilde{\Gamma}^{-1} \frac{2\alpha}{3\pi} \frac{1}{r} \left(1 + \frac{1r_i}{2r}\right) \left(1 - \frac{r_i}{r}\right)^{1/2} \\ &\cdot \left(\frac{1}{2}(1-r^2) + r \ln r\right) \end{aligned} \quad (6)$$

where  $\tilde{\Gamma}$  denotes the fully integrated RPA-rate normalized to the inclusive photon rate. The normalized total RPA-rate is given by

$$\begin{aligned} \tilde{\Gamma} &= \frac{2\alpha}{3\pi} \left[ -\frac{1}{2} \ln \frac{1 - \sqrt{1-r_i}}{1 + \sqrt{1+r_i}} (1 + 3r_i + \frac{3}{8}r_i^2) \right. \\ &\quad \left. - \frac{5}{12} \sqrt{1-r_i} (5 + \frac{1}{2}r_i) \right] \end{aligned}$$

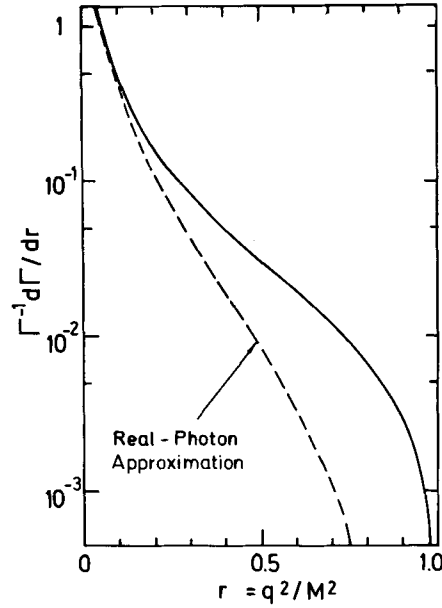


Fig. 2. Differential decay rate for  $\Psi \rightarrow e^+ e^- + gg$  normalized to 1. Dashed curve corresponds to Real-Photon-Approximation

$$\begin{aligned} &= \frac{2\alpha}{3\pi} \left[ -\frac{1}{2} \ln r_i - \frac{25}{12} + \ln 2 \right. \\ &\quad \left. - \frac{3}{2} r_i (\ln r_i + 1 - 2 \ln 2) + \dots \right] \end{aligned} \quad (7)$$

In Table 1 we give the results of the full rates normalized to the inclusive photon rate for the cases considered in this paper. The rates are down roughly by two orders of magnitude compared to the inclusive photon rate as one expects from the naive  $O(\alpha)$  estimate. The differences in rates for the various cases considered in Table 1 reflect the relative proximity of threshold to the photon pole in each case. That the rate is dominated by the contributions close to threshold is evidenced from the fact that the numbers in Table 1 are fairly well approximated by the RPA-rate (7) even though the differential RPA-rate is much smaller than the exact rate over much of the  $r$ -range (see Fig. 2). The other three cases  $\Psi \rightarrow \mu^+ \mu^- + gg$  and  $\Upsilon \rightarrow e^+ e^- (\mu^+ \mu^-) + gg$  can be easily obtained by rescaling Fig. 2. They only differ in shape close to threshold which is not resolved on the linear  $r$ -scale in Fig. 2. More details on the spin-averaged case

Table 1. The ratio  $\Gamma(Q\bar{Q}(1^{--}) \rightarrow 1^+ 1^- + gg) / \Gamma(Q\bar{Q}(1^{--}) \rightarrow \gamma + gg)$  for  $\Psi \rightarrow e^+ e^- (\mu^+ \mu^-)$  and  $\Upsilon \rightarrow e^+ e^- (\mu^+ \mu^-)$ . Numbers in brackets are for the Real-Photon-Approximation

	$e$	$\mu$
$\Psi$	$1.07 \times 10^{-2}$	$2.44 \times 10^{-3}$
	$(1.03 \times 10^{-2})$	$(2.07 \times 10^{-3})$
$\Upsilon$	$1.24 \times 10^{-2}$	$4.11 \times 10^{-3}$
	$(1.20 \times 10^{-2})$	$(3.75 \times 10^{-3})$

including the case of the  $\tau$ -lepton can be found in [1]. We shall now turn to the polar and azimuthal angular asymmetries.

### Polar Asymmetry

On  $x_q$ ,  $x_2$  and  $\varphi^*$ -integration one obtains from (1) the polar distribution of the lepton pair (Fig. 3) which we parametrize as usual as

$$\frac{d\Gamma}{dr d\cos\Theta^*} \sim 1 + \alpha(r) \cos^2\Theta^* \quad (8)$$

where  $(-1 \leq \alpha \leq 1)$

$$\alpha = \frac{\iint (\mathcal{H}_{\mu\mu} - 3\mathcal{H}_{00})(1 - r_t/r)}{\iint (\mathcal{H}_{\mu\mu} + \mathcal{H}_{00})(1 + r_t/r)} \quad (9)$$

In (9) we have indicated the  $x_q$  and  $x_2$  integration which are to be done in the limits (5).

The longitudinal component of the hadron tensor  $\mathcal{H}_{00}$  is given by

$$\mathcal{H}_{00} = H_1 - p_{2z}^* H_2 - p_{3z}^* H_3 - 2p_{2z}^* p_{3z}^* H_4$$

where  $p_{2z}^*$  and  $p_{3z}^*$  are the  $z$ -components of the gluon momenta 2 and 3 in the rest frame of the virtual photon. For gluon 2 this reads

$$p_{2z}^* = M(ax_q - 2x_2r)/(4r(x_q^2 - 4r))^{1/2} \quad (10)$$

and similarly for gluon 3 with  $2 \leftrightarrow 3$  and  $a \leftrightarrow b$ .

The analyzing power of the Dalitz pair is given by  $(1 - r_t/r)/(1 + r_t/r)$  which vanishes at threshold  $r = r_t$  due to  $s$ -wave threshold production. Over most of the range of  $r$  the analyzing power is well approximated by its zero lepton mass limit, namely 1. In Fig. 3 we have plotted the asymmetry in this limit. Note that the asymmetry then no longer depends on the quarkonium mass  $M$ . In the real photon limit  $r = 0$  the longitudinal component decouples and consequently one has  $\alpha = 1$  in this limit neglecting threshold effects. At the phase space limit  $r = 1$  the asymmetry goes to zero.

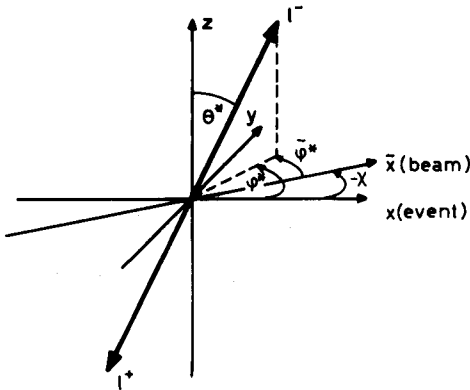


Fig. 3. Definitions of polar angle  $\Theta^*$  and azimuthal angles  $\varphi^*$  and  $\tilde{\varphi}^*$ .  $z$ -axis along momentum of virtual photon.  $(x - z)$ -plane is event plane and  $(\tilde{x} - z)$ -plane is  $(\gamma^*$ -beam)-plane. Relative orientation of the two planes given by  $-\chi$  in the notation of [4]

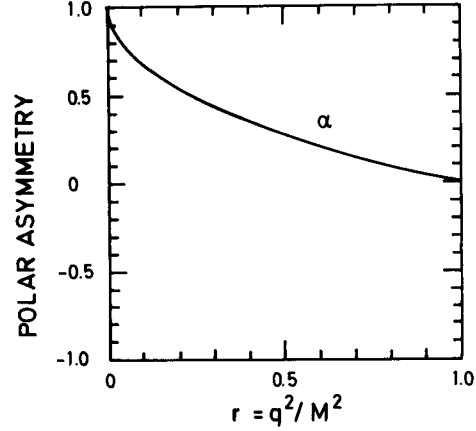


Fig. 4. Polar asymmetry

### Azimuthal Asymmetry

On  $x_q$ ,  $x_2$  and  $\cos\Theta^*$  integration one obtains from (1) the azimuthal distribution of the lepton pair which we parametrize as

$$\frac{d\Gamma}{dr d\varphi^*} \sim 1 + \beta(r) \cos 2\varphi^* \quad (11)$$

For the azimuthal asymmetry  $\beta$  one obtains  $(-\frac{1}{2} \leq \beta \leq \frac{1}{2})$

$$\beta = P_{\text{lin}} \cdot A = \left( - \frac{\iint 2\mathcal{H}_{+-}}{\iint \mathcal{H}_{\mu\mu}} \right) \frac{(-1 + r_t/r)}{(2 + r_t/r)} \quad (12)$$

where the linear polarization of the (virtual) photon is given by the bracket on the r.h.s. of (12). The analyzing power  $A$  of the Dalitz pair is  $(-1 + r_t/r)/(2 + r_t/r)$  which is zero at threshold, again for the reason that the Dalitz pair is created in an  $s$ -wave at threshold. The linear polarization of the virtual photon is determined by

$$\mathcal{H}_{+-} = \frac{1}{2} p_{2x}^* (H_2 + H_3 - 2H_4) N \quad (13a)$$

which reduces to

$$\mathcal{H}_{+-}(r=0) = 2N(r=0)(1 - x_q)(1 - x_2)(1 - x_3) \quad (13b)$$

in the limit  $r = 0$  in agreement with the results given in [3–5].  $p_{2x}^*$  is the transverse component of the momentum of gluon 2 in the virtual photon's rest frame (or in the overall c.m. frame)

$$p_{2x}^* = M^2(a(x_q x_2 - a) - r x_2^2)/(x_1^2 - 4r) \quad (14)$$

In Fig. 4 we plot the azimuthal asymmetry for the zero lepton mass limit, which again is a good enough approximation in the cases considered here over most of the range of  $r$ . The asymmetry is small and positive for small  $r$ -values and goes to zero at the phase space limit  $r = 1$ .

For a measurement of the azimuthal asymmetry it is experimentally advantageous to use the beam-virtual photon plane as a reference plane for the

azimuthal measurement (Fig. 3). Since information on the direction of the beam is transmitted by the spin 1 quarkonium state via its density matrix it is clear that one needs the full hadron tensor

$$\mathcal{H}_{\mu\nu\alpha\beta} = \sum_{\text{gluon spins}} A(Q\bar{Q}(\alpha) \rightarrow \gamma^*(\mu)gg) \cdot A^*(Q\bar{Q}(\beta) \rightarrow \gamma^*(\nu)gg)$$

in order to extract the desired information. As explained in more detail in [4] this is achieved by rotating  $P_{\text{lin}}$  to the beam-virtual photon plane and then integrating out the relative azimuthal  $\chi$ -dependence.

In this way one finds

$$\tilde{\beta} = \tilde{P}_{\text{lin}} \cdot A = \frac{\iint (-\mathcal{H}_{+-;+-})(-1+r_i/r)}{\iint (\mathcal{H}_{\mu\mu})} \frac{(2+r_i/r)}{(2+r_i/r)} \quad (15)$$

where  $\mathcal{H}_{+-;+-}$  is the appropriate helicity projection of the full hadron tensor  $\mathcal{H}_{+-;+-} = \varepsilon_\alpha(+)\varepsilon_\beta^*(-)\mathcal{H}_{\mu\nu\alpha\beta}e_\mu^*(+)\varepsilon_\nu(-)$ . One finds after some algebra

$$\mathcal{H}_{+-;+-} = A + Bp_{2x}^{*2} + Cp_{2x}^{*4} \quad (16a)$$

where

$$\begin{aligned} A &= 2[x_2x_3(ab-2rc) + 2r(1+r)c^2]N \\ B &= 2[-(1-r)(a^2+b^2-2rc) + 2c(rc-ab)]N/M^2 \\ C &= 2[(x_1-2r)^2]N/M^4 \end{aligned}$$

In the limit  $r=0$  one has

$$\mathcal{H}_{+-;+-} = 2N(r=0) \frac{(1-x_2)^2(1-x_3)^2}{x_q^2} \quad (16b)$$

which agrees with the result of [4].

For small  $r$ -values the beam-virtual photon plane azimuthal asymmetry  $\tilde{\beta}$  is smaller than the corresponding event plane asymmetry  $\beta$  but rises to quite large values as  $r$  approaches 1 (Fig. 5)

In order to assess the measurability of the proposed angular distributions we plot in Fig. 6 the percentage rate of events with a lab frame opening angle larger than a given opening angle. Depending on the granularity and dimensionality of the detector, opening angle cuts presumably are the most important cuts in reducing experimental event rates in such a measurement.

In Fig. 6 we include the cases  $\Psi \rightarrow e^+e^-(\mu^+\mu^-)$ ,  $\Upsilon \rightarrow e^+e^-(\mu^+\mu^-)$  and the hypothetical toponium state with a mass of 42 GeV  $T(42) \rightarrow e^+e^-(\mu^+\mu^-)$ . One notes that in the muon case the opening angle cuts do not remove a large fraction of the event sample, whereas in the electron case opening angle cuts can remove substantial fractions of the (theoretical) event rates depending of course on detector specifications.

As is well known the Ore-Powell spectrum peaks toward large photon energies. Thus the events with small opening angles are primarily populated by low-invariant mass lepton pairs close to their threshold. These are also the events where the analyzing power of the Dalitz pair is reduced from its maximum

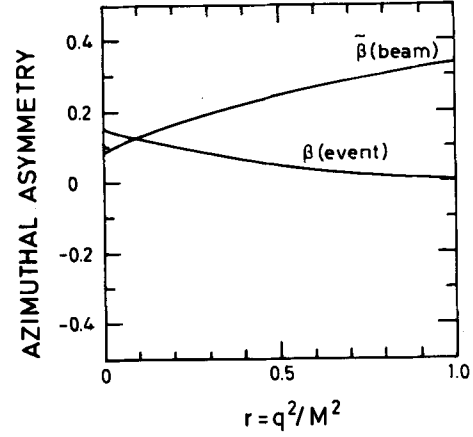


Fig. 5. Azimuthal asymmetry  $\beta$  and  $\tilde{\beta}$  for the two azimuthal reference planes as explained in caption of Fig. 3

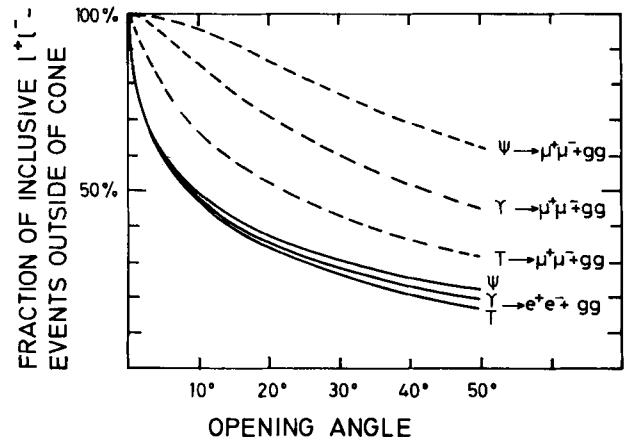


Fig. 6. Percentage rate of events with lab frame opening angle larger than a given angle. Each curve based on 500 K MC events

values 1 and  $-0.5$  (12) and (15) for the polar and azimuthal distributions, respectively. One concludes that opening angle cuts enhance the sample with events close to their maximal analyzing power. This problem can be studied in more detail in Monte Carlo simulations.

The present investigation originated in the question whether it was feasible to measure the linear polarization of an inclusive photon from heavy quarkonium decay through Dalitz pair creation [5]. It had been noted that the analyzing power of Dalitz-pairs by far exceeds the analyzing power of Bethe-Heitler pairs, which, although possibly higher in rate, suffer from theoretical uncertainties in their analysis as well from the fact that the opening angle of the Bethe-Heitler pairs originating from high energy photons is quite small.

Assuming that experimental conditions allow one to usefully sample  $\sim 25\%$  of the theoretically predicted lepton pair rates of Table 1 one expects to see  $\sim 10^{-4}$   $e$ -pairs and  $\sim 4 \times 10^{-5}$   $\mu$ -pairs from each  $\Upsilon$ -decay. With present luminosities at DORIS 2 and CESR

production rates of  $\sim 10^{-5} \gamma$ 's/month appear feasible. Thus the proposed measurements are within reach of present experiments. Using the same 25% reduction factor one has for every  $\Psi$ -decay  $\sim 4 \times 10^{-4}$  inclusive  $e$ -pairs and  $\sim 10^{-4}$   $\mu$ -pairs. These rates are large enough to attempt an analysis on already existing data ( $\sim 3 \times 10^6 \Psi$ 's). Although it is not clear whether the mass of the  $\Psi$  is sufficiently high to trust the detailed results of a perturbative QCD calculation it is nevertheless interesting to compare data with the averaged angular asymmetries presented in this paper.

*Acknowledgements.* We would like to thank Y. Zaitsev, W. Schmidt-Parzeval, J. Willrodt and L. Jones for discussions and for

encouragement. This work was begun while D. McKay was a Humboldt Fellow visiting at the II. Institute of Theoretical Physics of the University of Hamburg. D. McKay would like to thank the Humboldt-Foundation for support and Prof. G. Kramer for hospitality.

## References

1. J.P. Leveille, D.M. Scott: Phys. Lett. **95B**, 96 (1980)
2. Z. Kunszt, H.R. Rubinstein: Phys. Lett. **80B**, 129 (1978); H. Fritzsch, K.H. Streng: Phys. Lett. **77B**, 299 (1978)
3. S.J. Brodsky, T.A. deGrand, R.F. Schwitters: Phys. Lett. **79B**, 255 (1978)
4. J.G. Körner, D.H. Schiller: DESY-Preprint 81-043 (1981)
5. J.G. Körner, D. McKay: Z. Phys. C—Particles and Fields **9**, 67 (1981)